Journal of Power Sources 453 (2020) 227906

Contents lists available at ScienceDirect

Journal of Power Sources

journal homepage: www.elsevier.com/locate/jpowsour

Overestimation of biofilm conductance determined by using the split electrode as the microbial respiration

Panpan Liu [a], Peng Liang [a,*], Haluk Beyenal [b,**], Xia Huang [a]

[a] State Key Joint Laboratory of Environment Simulation and Pollution Control School of Environment, Tsinghua University, Beijing, 100084, PR China
[b] The Gene and Voiland School of Chemical Engineering and Bioengineering, Washington State University, Pullman, WA, 99163, USA

HIGHLIGHTS

- Biofilm conductance decreased with current production as consumption of substrate.
- Biofilm conductance increased with the area of drain electrode.
- The measurement of biofilm conductance was influenced by microbial metabolism.
- Biofilm conductance significantly decreased under non-turnover condition.

ARTICLE INFO

Keywords:
Biofilm conductance
Extracellular electron transfer
Geobacter sulfurreducens
Bioelectronics
Microbial electrochemistry

ABSTRACT

Advancing the application of bioelectrochemical systems necessitates the comprehensive understanding of electron transfer process in electrode-associated biofilm. While *in situ* electrical measurement by using the split electrode can illustrate the electron conduction in biofilm, the accuracy and interpretation of the obtained data is still in debate. Here, conductance of *Geobacter sulfurreducens* biofilm is measured by using the split electrode as substrate concentration is changed. Biofilm conductance decreases with the current production as the consumption of substrate. In addition, the measured conductance increases with the area of drain electrode (13.8 ± 1.8 μS for 0.5 cm^2 and 29.4 ± 4.2 μS for 1 cm^2). These results suggest the measured conductance of biofilm is influenced by microbial metabolism. This effect will diminish when the measurement is performed by using electrochemical impedance spectroscopy or under non-turnover condition. Our results provide the insight on the electrochemical origin of biofilm conductance determined by the *in situ* electrical measurement.

1. Introduction

The ability of electrochemically active bacteria to deliver intercellular metabolic electrons to extracellular solid electrode shows promise for recovering value-added products from organic matter and wastewater in bioelectrochemical systems (BES) [1–3]. Electron transport from bacteria to solid electrode outside the cell, known as extracellular electron transport (EET), serves as the fundamental working principles of BES. Bacteria in BES always attached to the electrode and assembled into electrochemically active biofilm (EAB). High current density greatly depend on the EET in EAB and is essential for the application of BES [4,5]. However, the mechanism of the electron conduction in EAB is not fully understood as the complex process was mediated by various electrochemical components including conductive filaments [6,7], extracellular cytochromes [8,9], redox shuttles [10], or their combination [11–13].

Apparent conductance determined by *in situ* electrical measurements on living EAB had been used to illustrate the mechanism of electron conduction in biofilm [14]. While the observed conductance of biofilm was significantly different under various conditions, e.g. with/without substrate oxidation [15,16], different buffer concentration [17] and varied electrode potentials [18,19]. Accordingly, these results had been interpreted by the different mechanisms of electron conduction in biofilm. For the model *Geobacter sulfurreducens* biofilm, the dependence of biofilm conductance on electrode potential was interpreted by two conflicting models: incoherent redox conductivity mediated by outer

* Corresponding author. State Key Joint Laboratory of Environment Simulation and Pollution Control School of Environment, Tsinghua University, Beijing, 100084, PR China.
** Corresponding author. The Gene and Voiland School of Chemical Engineering and Bioengineering, Washington State University, Pullman, WA, 99163, USA
E-mail addresses: liangpeng@tsinghua.edu.cn (P. Liang), beyenal@wsu.edu (H. Beyenal).

https://doi.org/10.1016/j.jpowsour.2020.227906
Received 12 November 2019; Received in revised form 21 January 2020; Accepted 14 February 2020
Available online 5 March 2020
0378-7753/

membrane c-type cytochromes [19,20] and intrinsic metallic-like conductivity through the electron delocalized occurring on the π−π stacking of aligned aromatic moieties in conductive e-pili [18]. These two distinct difference models might insinuate complex electroactive matrix involved in the electron transport in biofilm.

Electrical measurements are based on the assumption that the conductivity can be calculated from the measured electron transport across the biofilm bridging the non-conductive gap [15,21]. The measured electron transport involved at least two processes: heterogeneous electron transfers across biofilm-electrode interface and homogeneous electron transfer in biofilm not in direct contact the electrode surface [22]. Extracellular respiration of electrode by *G. sulfurreducens* biofilm is one of metabolism process of by *G. sulfurreducens* biofilm. This special respiration allowed the exchange of electrons between the electrode and biofilm [23]. However, it is still unknown whether the effect of this respiration is involved in these processes of electron transport. As a consequence, the observed conductance might be affected by the respiration of biofilm and the mechanism of EET in biofilm elucidated from these *in situ* electrical measurements might need to be revisited.

In order to get the comprehensive understanding of electron conduction in EAB, *in situ* electrical measurements on living *Geobacter sulfurreducens* biofilm are performed by using the split electrode which comprises a pair of gold electrode (source electrode and drain electrode) with a non-conductive gap between them. Effects by the biofilm respiration on the electrical measurements were investigated by varying the electrode areas and substrate concentration. In addition, biofilm resistance was determined simultaneously by using electrochemical impedance spectroscopy. Comparison of these results could elucidate the electrochemical origin of the observed conductance of *G. sulfurreducens* biofilm.

2. Method and materials

2.1. Fabrication of split electrode

Split electrode was fabricated by adapting previous report [24]. Briefly, Ti and Au layer were patterned onto the surface of a clean glass wafer and the 20 μm non-conductive gap was defined by using the electron-beam lithography. The thicknesses of Ti and Au layers were 20 nm and 200 nm, respectively [20]. The size of *G.sulfurreducens* is about 1–2 μm and it was ten-fold bigger than that of Ti/Au layer [25]. The split electrode (0.5 cm × 1 cm) comprised four separated electrodes (which designated as A, B, C and D) and three non-conductive gaps (Fig. 1). The electrode part was covered with Ti/Au layer while the gap part was not covered with Ti/Au layer. Each electrode was wired with copper conductor by soldering them together with 60:40 tin/lead, respectively. All copper conductors were wrapped in insulated polyvinyl chloride (PVC). A layer of silicone gel covered the connect joints to eliminated the corrosion by electrolyte. Bare copper wire near the connect joints was also covered by the silicone gel. Before placed into reactor, the whole electrode was thoroughly cleaned with DI water.

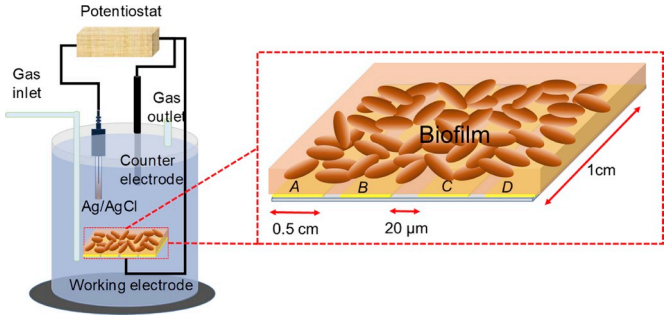

Fig. 1. Schematic illustration of the setup of reactor used to grow biofilm and the geometry of split electrode.

2.2. Growth of G. sulfurreducens biofilm

G. sulfurreducens strain PCA (ATCC 51573) was firstly grown anaerobically in serum vial at 30 °C for approximately 3 days. The growth medium contained (1L): KCl, 0.38 g; NH_4Cl, 0.2 g; Na_2HPO_4, 0.069 g; $CaCl_2$, 0.04 g; $ZnSO_4{\cdot}7H_2O$, 0.2 g; $NaHCO_3$, 2 g; Wolfe's vitamin solution, 10 mL; modified Wolfe's mineral solution, 10 mL, 1.64 g sodium acetate and 6.4 g sodium fumarate.

G. sulfurreducens biofilm was grown at 30 °C in a batch reactor with a volume of 125 mL (Fig. 1). The reactor was made of glass and anaerobic condition was maintained by bubbling the N_2/CO_2 (80%/20%) mixing gas continually by using the tygon tube (Cole-Parmer, Vernon Hills, IL, catalog EW-06475-14, EW-06475-16) with a 0.2-mm filter. Before inoculum, the mix gas was bubbled for at least 24 h to remove the trace oxygen in the reactor and medium. Then 10 mL G. *sulfurreducens* strain solution was injected into the reactor. The growth medium was used as described above but omitting the sodium fumarate. Biofilm was grown on the split electrode with the polarized potential of +0.2 V vs. Ag/AgCl which was controlled by using a custom-made potentiostat. The value of +0.2 V vs. Ag/AgCl was chosen according to previous studies [20,26]. A Ag/AgCl and graphite rod were used as the reference electrode and counter electrode, respectively.

2.3. In situ electrical measurements of G. sulfurreducens biofilm

All the electrical measurements were performed with the Gamry 300™ potentiostat (Gamry Instruments, Warminster, PA). Cyclic voltammetry (CV) of biofilm was conducted with three-electrode system, in which split electrode attached with biofilm was used as working electrode while Ag/AgCl and graphite rod was used as reference and counter electrode. The potential scanned from −0.7 V vs. Ag/AgCl to +0.4 V vs. Ag/AgCl at a rate of 10 mV/s. The complete substrate-depleted condition (non-turnover condition) was obtained by polarizing the working electrode at +0.2 V vs. Ag/AgCl for 48 h after replacing the electrolyte with fresh medium without any electron donor and acceptor. After the current production of biofilm was below 2 μA, CVs of biofilm was performed by scanning the potential from −0.7 V vs. Ag/AgCl to +0.4 V vs. Ag/AgCl with varied scan rate of 1 mV/s to 100 mV/s.

To measure the conductance of the biofilm bridging the non-conductive gap, electrode on the one side of the gap was used as source electrode and the other side was used as the drain electrode. A voltage difference (U_{SD}, 0 mV, 25 mV, or 50 mV) was applied to the gaps. For each voltage, a long period of 5 min was applied to allow the transient current to decay. Current (I_{SD}) was recorded every second over the 5-min period, and the conductance of the biofilm was calculated using the values I_{SD} with U_{SD}. The impact of substrate concentration on biofilm conductance was evaluated by the electrical measurement performed during substrate consumption. Replacing the medium with fresh growth medium or adding the sodium acetate directly to recover the concentration of substrate. Area of source and drain electrode (A_{source} and A_{drain}) was varied by changing the number of connecting electrode used as the source electrode and the drain electrode. Results performed on gap with source electrode//drain electrode of B//C, (B)//(C + D), (A + B)//(C), and (A + B)//(C + D) represented the ratio of A_{source}: A_{drain} of 0.5 cm^2//0.5 cm^2, 0.5 cm^2//1.0 cm^2, 1.0 cm^2//0.5 cm^2 and 1.0 cm^2//1.0 cm^2, respectively (Fig. S1).

Electrochemical Impedance Spectroscopy (EIS) conducted on the biofilm bridging the gap with the source electrode as the working electrode, and the drain electrode as the reference and counter electrode. The applied AC potential was 10 mV rms and the frequency range was from 100 mHz to 100,000 Hz with 10 points of data acquisition. Zview software (Scribner Associates Inc., Southern Pines, NC, USA) was used to analyze biofilm impedance obtained from EIS results.

2.4. Confocal imaging of G. sulfurreducens biofilm

Images of *G. sulfurreducens* biofilm was obtained by using a Nikon C1 confocal microscope (Eclipse TE200, Nikon, Tokyo, Japan) with a 10 × objective lens. The whole electrode covered with *G. sulfurreducens* biofilm first stained with a live/dead BacLight Bacterial Viability Kit (Molecular Probes, Eugene, OR, USA) following the instructions of the manufacturer. The obtained images were processed by using the NIS-element software (Nikon, Tokyo, Japan).

3. Results

3.1. Biofilm conductance changing with current production

Current production of working electrode and conductance of biofilm increased with inoculum time, suggested biofilm grew on the electrode (Fig. S2A). The confocal image confirmed the biofilm growth across the non-conductive gaps (Fig. S2B). Mature *G. sulfurreducens* biofilm with the stable current production was selected to investigate its conductance changed with the medium replacement. The stable current production by *G. sulfurreducens* biofilm was 1.04 ± 0.03 A/m^2 in first four days of selected period and the biofilm conductance was 13.3 ± 1.3 μS (Fig. 2) at the selecting day. The consumption of substrate led to the decrease of current production and the conductance decreased correspondingly (Fig. S2A). At 6th day, the current production and conductance of biofilm decreased to 0.67 A/m^2 and 10.3 ± 1.1 μS, respectively. After replacing the electrolyte with fresh substrate medium, current production immediately increased and recover to 1.03 ± 0.05 A/m^2 in four days. Biofilm conductance was also getting back to 12.8 ± 1.1 μS at 11th day. Interestingly, Higher biofilm conductance (10.3 ± 1.1 μS) was observed at 6th day before the replacement of medium compared with that after the replacement (6.1 ± 1.8 μS) at 9th day, even though the same current (0.67 A/m^2) was produced by the biofilm under these two conditions. This difference might be caused by the remove of electroactive components in the electrolyte after replacing it with fresh medium. Further experiment was used to verify this speculation. At 20th day, substrate concentration was recovered by adding 0.2 g sodium acetate into the electrolyte directly. Same conductance (10.6 ± 1.8 μS) of biofilm collaborated with the current production (0.67 A/m^2) either before or after adding the sodium acetate, indicating that the electroactive components in electrolyte could affect the measurements of biofilm conductance.

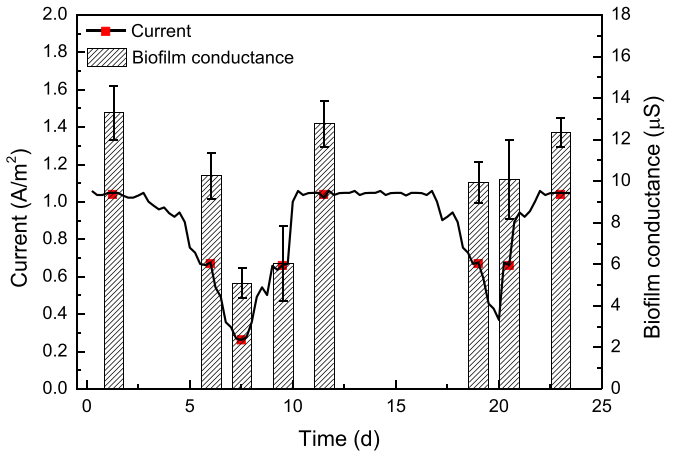

Fig. 2. Current production of *G. sulfurreducens* biofilm and the biofilm conductance changing with substrate concentration.

3.2. Different biofilm conductance and resistance obtained with varying electrode area

Results from electrical measurements based on direct current method and EIS were used to calculate the biofilm conductance and the total resistance (R_{total}) of biofilm (Fig. S3). During these tests, there was sufficient substrate in the medium and the change of physicochemical property of medium was small. The biofilm structure did not change and the obtained results can reflect the effect of electrode area on conductance measurement. Fig. 3 shows the conductance and resistance ($R_{biofilm}$) of biofilm bridging gap with varying the area of source electrode (A_{source}) and drain electrode(A_{drain}). Increasing A_{drain} led to the increase of biofilm conductance, which was 13.8 ± 1.8 μS ((B)//(C)), 14.6 ± 3.2 μS ((A + B)//(C)) for the A_{drain} of 0.5 cm^2 comparing to 29.4 ± 4.2 μS ((B)//(C + D)), 32.8 ± 1.2 μS ((A + B)//(C + D)) for A_{drain} of 1 cm^2. This difference revealed that the measurement of biofilm conductance is significantly affected by the area of drain electrode. Interestingly, biofilm conductance obtained with (B)//(C + D) (14.6 ± 3.2 μS) was about 2-fold smaller than that obtained with (A + B)//(C) (29.4 ± 4.2 μS). This difference suggested that the measured biofilm conductance was depended on the area of drain electrode. Biofilm resistance ($R_{biofilm}$) obtained from EIS coupled with equivalent circuit analysis (Fig. S4) also changed with the area of source and drain electrode (Fig. 2). The smallest $R_{biofilm}$ was 63.4 ± 1.9 kΩ for biofilm with (A + B)//(C + D), comparing with that with (B)//(C) (88.3 ± 2.0 kΩ), (B)//(C + D) (92.4 ± 3.1 kΩ) and (A + B)//(C) (85.5 ± 2.1 kΩ). This result suggested that $R_{biofilm}$ obtained by EIS was depended on the smaller one between A_{source} and A_{drain}.

3.3. Biofilm conductance and resistance obtained under non-turnover condition

After long period of starvation and polarization, current produced by biofilm was below 2 μA and the measured conductance showed in Fig. 4A. Varying electrode area did not significantly influence the obtained biofilm conductance, which was 3.3 ± 0.1 μS for (B)//(C), 3.7 ± 0.3 μS for (A + B)//(C), 3.4 ± 0.2 μS for (B)//(C + D) and 3.8 ± 0.3 μS for (A + B)//(C + D). In addition, biofilm conductance significantly decreased from 13.3 μS ((B)//(C)) with substrate oxidation to 3.3 μS without substrate oxidation. These results suggested that the measurement of biofilm conductance might be influenced by microbial metabolism. Moreover, EIS measurement revealed the similar biofilm resistance ($R_{biofilm}$) even with different area of source/drain electrode (360.3 ± 5.0 kΩ for (B)//(C), 347.3 ± 3.9 kΩ for (A + B)//(C), 353.3 ± 4.6 kΩ for (B)//(C + D), and 350.3 ± 6.1 kΩ for (A + B)//(C + D)). Under non-turnover condition, the typical non-turnover CVs in Fig. S5

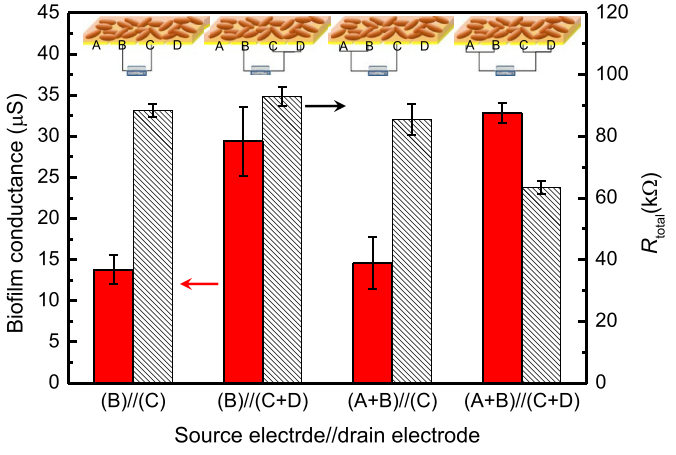

Fig. 3. Conductance and impedance of biofilm with varying ratios of the source and drain electrode area.

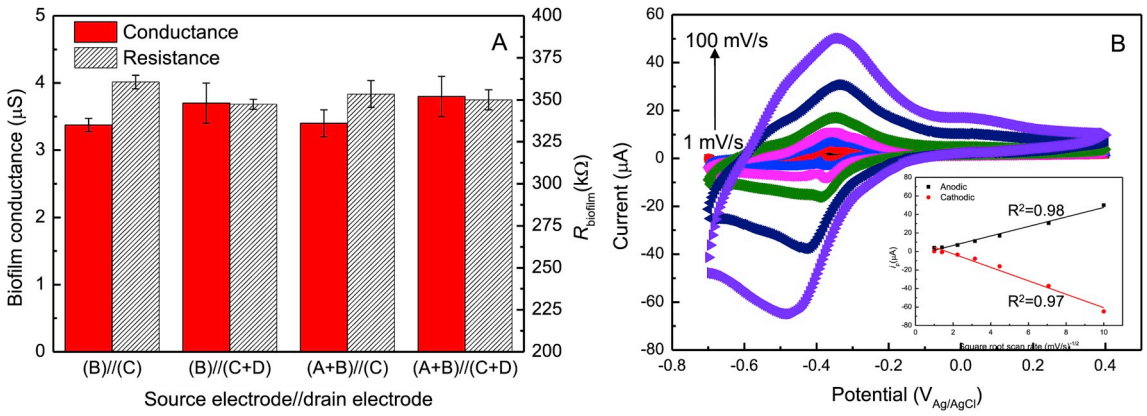

Fig. 4. (A) Conductance and impedance of biofilm under non-turnover condition. (B) CVs of biofilm with different scant rates under non-turnover condition, inset is the linear relationship between the peak current and the square root of scan rates.

and Fig. 4B were obtained for biofilm. The height of reversible peaks near −0.35 V vs. Ag/AgCl in the forward and backward scan revealed a linear dependence on the square root of the scan rate ranging from 1 mV/s to 100 mV/s. This relationship clearly revealed the diffusion-like behavior of electron transfer in *G. sulfurreducens* biofilm, which can be mediated by the collision or inter-protein reactions of bound redox molecules [19].

4. Discussion

The measured biofilm conductance depended on the current production and the area of source and drain electrode, indicating *in situ* electrical measurement of biofilm conductance was influenced by microbial metabolism. Fig. 5 schematically illustrate the electrochemical origins of measured current determined by *in situ* electrical measurement. The measured current comes from two types of electron flows including the electron produced by microbial metabolism coupling with the ionic transport current and the electron transport through the biofilm bridging the gap. Under the turnover condition, electrons uptake by drain electrode with larger area could led to 2.3-fold increase of measured current and result in high biofilm conductance (13.8 ± 1.8 μS and 29.4 ± 4.2 μS for the A_{drain} of 0.5 and 1 cm^2, respectively). However, doubling the area of source electrode did not lead the increase in the observed biofilm conductance (Fig. 3). This difference might be due to the unfeasible uptake/store of electrons by bacteria with the substrate oxidation. Under turnover condition, the current produced by biofilm (~52.1 μA) of source electrode was far greater than the measured current (~0.7 μA). Increasing the area of source electrode did not significantly increase the measured biofilm conductance (Fig. 3). While the uptake/store of electrons by biofilm was unfeasible and increasing the area would lead a higher metabolic current on drain electrode. Then the measured biofilm conductance increased with the area of drain electrode. In addition, the uptake/store of electrons by suspend bacteria also influenced the measurement of biofilm conductance. Reserving suspend bacteria by adding sodium acetate after the consumption of substrate could led to the faster recovery of biofilm conductance than replacing the entire medium (Fig. 2).

The result that measured current included electron produced by microbial metabolism would led the overestimation of biofilm conductance and the inaccuracy of electron conduction mechanism obtained by *in situ* electrochemical gating measurement. When electrochemical gating measurement was conducted without the counter electrode to

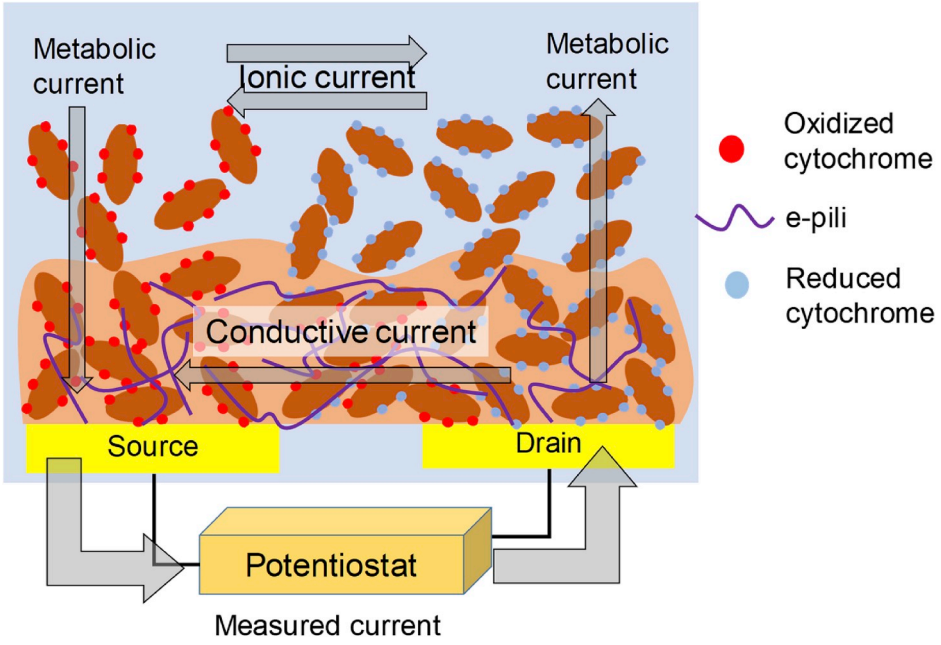

Fig. 5. Schematic illustration of the electrical conductance measurement by using the split electrode.

accept the electron produced by microbial metabolism (Fig. S6A), the obtained biofilm conductance increased with the electrode potential [18]. Accordingly, the metallic-like mechanism of electron conduction was proposed to character electron transfer in *G. sulfurreducens* biofilm [18]. However, conducting electrochemical gating measurement with biopotentiostat can allow metabolic electron flow to the counter electrode (Fig. S6B) and a maximum conductance of biofilm was obtained at the potential of −0.4 V vs. Ag/AgCl. As a result, electron transfer in *G. sulfurreducens* biofilm was considered as redox-type electron conduction [19,20]. The non-turnover CVs of biofilm with different scan rates also revealed the redox-type electron transfer in biofilm (Fig. 4B). Furthermore, the redox-type conduction mechanism was supported by results obtained from spectroelectrochemical measurement including surface-enhanced Raman spectroscopy [27] and UV/Vis spectroscopy [28].

The effect of microbial metabolism on the measurement of biofilm conductance can be eliminated by omitting substrate completely. Under non-turnover condition, the observed biofilm conductance would independent on the electrode area (Fig. 4A). However, the inhibition of microbial activity might have an effect on the biofilm structure and impede electron transfer in biofilm. These effects could lead to the underestimation of biofilm conductance [16]. Alternatively, EIS measurement was proposed to determine the biofilm resistance. When coupling with equivalent circuit fitting, EIS measurement could distinguish the conductive impedance from the total impedance. Small difference (~8%) of obtained $R_{biofilm}$ for biofilm with different area of source or drain electrodes was obtained under turnover condition (Fig. 3), indicating EIS measurement was not influenced by microbial metabolism. But significantly decrease (~26%) of $R_{biofilm}$ was obtained for (A + B)//(C + D) (Fig. 3). This difference indicated that $R_{biofilm}$ obtained by EIS measurement depended on reactions occurring on the source and drain electrode simultaneously. Further *in situ* electrochemical on conductive biofilm should pay attention to electrode distance/area dependence [24].

Significant difference of $R_{biofilm}$ under turnover (88.3 ± 2.0 kΩ for (B)//(C)) and non-turnover conditions (360.3 ± 5.0 kΩ) was observed by EIS measurement. In addition, biofilm conductance obtained by using direct current method under turnover condition (13.3 μS) was much bigger than that under non-turnover conditions (3.3 μS). These differences indicated microbial activity influenced the electron transfer in biofilm. The cytochrome mediating electron transfer in biofilm depend on the reduced and oxidized of cytochrome, which altered with the varying metabolic activity of *G. sulfurreducens* [17,29]. Although conductive e-pili mediated electron transfer in *G. sulfurreducens* biofilm, it was previously supposed to work coordinately with the cytochromes as electron mediator to delivery electron in biofilm [11,30]. Moreover, the cytochrome (OmcZ) stacked structure of e-pili also could support the loss of biofilm conductance as the decrease of microbial metabolic activity [7]. Furthermore, the ability of electron delivery by cytochrome/nanowire was influenced by local microenvironments (i.e. pH and ORP) in biofilm which would change as the remove of substrate completely [31–33]. This affect also would lead the significant decrease of biofilm conductance under non-turnover condition.

5. Conclusion

In conclusion, conductance of *G. sulfurreducens* biofilm determined by using split electrode was significantly influenced by biofilm respiration. Under turnover condition, As the uptake of electron by biofilm, higher conductance was obtained by with the A_{drain} of 1 cm^2 (29.4 ± 4.2 μS) than that of 0.5 cm^2 (13.8 ± 1.8 μS). Using EIS measurement or removing the substrate completely can eliminate the influence of microbial metabolism on the determination of biofilm conductance. Significant decrease of biofilm conductance and $R_{biofilm}$ was observed under non-turnover condition (3.4 μS and 360.3 kΩ) compared with that under turnover condition (13.3 μS and 88.3 kΩ). This difference implied significance of cytochrome delivering electrode transfer in *G. sulfurreducens* biofilm. Our result suggested that the interpretations made in earlier experimental and theoretical studies should be revisited, particularly paying attention to the effect by the microbial respiration.

Declaration of competing interest

The authors declare that they have no known competing financial interests or personal relationships that could have appeared to influence the work reported in this paper.

Acknowledgements

This work was supported by the National Nature Science Foundation of China (NSFC No. 51778324, 51422810) and NSF award #1706889 (National Science Foundation, United States).

Appendix A. Supplementary data

Supplementary data to this article can be found online at https://doi.org/10.1016/j.jpowsour.2020.227906.

References

[1] C. Santoro, C. Arbizzani, B. Erable, I. Ieropoulos, J. Power Sources 356 (2017) 225–244.
[2] A. Kumar, L.H.-H. Hsu, P. Kavanagh, F. Barrière, P.N.L. Lens, L. Lapinsonnière, J. H. Lienhard V, U. Schröder, X. Jiang, D. Leech, Nat Rev Chem. 1 (2017), 0024.
[3] Y. Jiang, H.D. May, L. Lu, P. Liang, X. Huang, Z.J. Ren, Water Res. 149 (2019) 42–55.
[4] J. Babauta, R. Renslow, Z. Lewandowski, H. Beyenal, Biofouling 28 (2012) 789–812.
[5] P. Liu, P. Liang, Y. Jiang, W. Hao, B. Miao, D. Wang, X. Huang, Appl. Energy 216 (2018) 382–388.
[6] D.R. Lovley, Curr Opin Electrochem 4 (2017) 190–198.
[7] F. Wang, Y. Gu, J.P. O'Brien, S.M. Yi, S.E. Yalcin, V. Srikanth, C. Shen, D. Vu, N. L. Ing, A.I. Hochbaum, E.H. Egelman, N.S. Malvankar, Cell 177 (2019) 361–369 e310.
[8] L. Shi, H. Dong, G. Reguera, H. Beyenal, A. Lu, J. Liu, H.Q. Yu, J.K. Fredrickson, Nat. Rev. Microbiol. 14 (2016) 651–662.
[9] N.S. Malvankar, M.T. Tuominen, D.R. Lovley, Energy Environ. Sci. 5 (2012).
[10] Y. Xiao, E. Zhang, J. Zhang, Y. Dai, Z. Yang, H.E.M. Christensen, J. Ulstrup, F. Zhao, Sci Adv 3 (2017), e1700623.
[11] R.J. Steidl, S. Lampa-Pastirk, G. Reguera, Nat. Commun. 7 (2016) 12217.
[12] R. Renslow, J. Babauta, A. Kuprat, J. Schenk, C. Ivory, J. Fredrickson, H. Beyenal, Phys. Chem. Chem. Phys. 15 (2013) 19262–19283.
[13] M.V. Ordóñez, G.D. Schrott, D.A. Massazza, J.P. Busalmen, Energy Environ. Sci. 9 (2016) 2677–2681.
[14] N.S. Malvankar, M.T. Tuominen, D.R. Lovley, Energy Environ. Sci. 5 (2012) 5790.
[15] C. Li, K.L. Lesnik, Y. Fan, H. Liu, PloS One 11 (2016), e0155247.
[16] B.R. Dhar, H. Ren, J. Chae, H.-S. Lee, J. Power Sources 402 (2018) 198–202.
[17] B.R. Dhar, J. Sim, H. Ryu, H. Ren, J.W. Santo Domingo, J. Chae, H.S. Lee, Water Res. 127 (2017) 230–238.
[18] N.S. Malvankar, M. Vargas, K.P. Nevin, A.E. Franks, C. Leang, B.C. Kim, K. Inoue, T. Mester, S.F. Covalla, J.P. Johnson, V.M. Rotello, M.T. Tuominen, D.R. Lovley, Nat. Nanotechnol. 6 (2011) 573–579.
[19] M.D. Yates, J.P. Golden, J. Roy, S.M. Strycharz-Glaven, S. Tsoi, J.S. Erickson, M. Y. El-Naggar, S. Calabrese Barton, L.M. Tender, Phys. Chem. Chem. Phys. 17 (2015) 32564–32570.
[20] P. Liu, A. Mohamed, P. Liang, H. Beyenal, Bioelectrochemistry 131 (2020) 107395.
[21] M.D. Yates, S.M. Strycharz-Glaven, J.P. Golden, J. Roy, S. Tsoi, J.S. Erickson, M. Y. El-Naggar, S.C. Barton, L.M. Tender, Nat. Nanotechnol. 11 (2016) 910–913.
[22] M.D. Yates, B.J. Eddie, N. Lebedev, N.J. Kotloski, S.M. Strycharz-Glaven, L. M. Tender, Bioelectrochemistry 119 (2018) 111–118.
[23] J.A. Gralnick, H. Vali, D.P. Lies, D.K. Newman, Proc. Natl. Acad. Sci. U. S. A. 103 (2006) 4669–4674.
[24] M. Ding, H.Y. Shiu, S.L. Li, C.K. Lee, G. Wang, H. Wu, N.O. Weiss, T.D. Young, P. S. Weiss, G.C. Wong, K.H. Nealson, Y. Huang, X. Duan, ACS Nano 10 (2016) 9916–9926.

[25] K. Inoue, C. Leang, A.E. Franks, T.L. Woodard, K.P. Nevin, D.R. Lovley, Environ Microbiol Rep 3 (2011) 211–217.
[26] J. Wei, P. Liang, X. Cao, X. Huang, Environ. Sci. Technol. 44 (2010) 3187–3191.
[27] D. Millo, F. Harnisch, S.A. Patil, H.K. Ly, U. Schroder, P. Hildebrandt, Angew Chem. Int. Ed. Engl. 50 (2011) 2625–2627.
[28] Y. Liu, H. Kim, R.R. Franklin, D.R. Bond, ChemPhysChem 12 (2011) 2235–2241.
[29] N. Lebedev, S.M. Strycharz-Glaven, L.M. Tender, ChemPhysChem 15 (2014) 320–327.
[30] N.L. Ing, T.D. Nusca, A.I. Hochbaum, Phys. Chem. Chem. Phys. 19 (2017) 21791–21799.
[31] J.T. Babauta, H. Beyenal, Biotechnol. Bioeng. 111 (2014) 285–294.
[32] J. Hou, Z. Liu, Y. Zhou, W. Chen, Y. Li, L. Sang, Electrochim. Acta 251 (2017) 187–194.
[33] B.G. Lusk, I. Peraza, G. Albal, A.K. Marcus, S.C. Popat, C.I. Torres, J. Am. Chem. Soc. (2018).